
The Surface Hydro-Oxidation of LaNiO_{3-x} Thin Films

S. MICKEVIČIUS^{a,*}, S. GREBINSKIJ^a, V. BONDARENKA^a,
V. LISAUSKAS^a, K. ŠLIUŽIENĖ^a, H. TVARDAUSKAS^a,
B. VENGALIS^a, B.A. ORŁOWSKI^b, V. OSINNIY^b AND W. DRUBE^c

^aSemiconductor Physics Institute, A. Gostauto 11, 01108 Vilnius, Lithuania

^bInstitute of Physics, Polish Academy of Sciences

al. Lotników 32/46, 02-668 Warsaw, Poland

^cHamburger Synchrotronstrahlungslabor HASYLAB

am Deutschen Elektronen-Synchrotron DESY

Notkestr. 85, 22603 Hamburg, Germany

(Received July 3, 2007)

The high-energy X-ray photoelectron spectroscopy was used to determine the composition and chemical structure of epitaxial LaNiO_{3-x} films obtained by a reactive dc magnetron sputtering. It was found that the oxide and hydroxide species of La and Ni are on the films surface. The thickness of hydroxide enriched layer, estimated from the oxide and hydroxide peak intensities, is about 2 nm.

PACS numbers: 79.60.-i, 71.20.Nr, 29.20.Lq

1. Introduction

LaNiO_3 is one of the few conductive oxides with a crystal structure suitable for integration in epitaxial heterostructures with perovskites of enormous technological potential such as colossal magnetoresistance materials, high-temperature superconductors, and ferroelectrics. It is known that the considerable surface segregation of elements may take place in LaNiO_{3-x} samples [1]. Another factor to be considered is the tendency of rare earth oxides to absorb water vapor and carbon dioxide from air, so that any *ex situ* exposure of these films to air will result in an uncontrolled reaction and surface stoichiometry [2]. In the previous paper [3]

*corresponding author; e-mail: sigism@pf.lit

it was shown that even the short time (about two hours) exposure to an outside ambient leads to the formation of the hydroxide layer on the film surface.

X-ray photoelectron spectroscopy (XPS) using laboratory X-ray sources ($h\nu < 1500$ eV) is known as the surface analysis method (scanning depth ≈ 2 nm), which provides the direct information on the species relative concentration and their valence states. On the other hand, synchrotron X-rays at much higher energies are used to significantly enhance the scanning depth. In this paper we utilize the volume sensitivity of tuneable high-energy XPS to study the epitaxial LaNiO_{3-x} films after long time (about one year) aging in air atmosphere.

2. Experimental

LaNiO_{3-x} thin (≈ 0.1 μm) films were obtained by using a reactive DC magnetron sputtering technique. Epitaxial LaNiO_{3-x} films deposited onto (100)-plane oriented NdGdO_3 substrate demonstrate the excellent in-plane orientation [4] and the surface La/Ni ratio is close to the bulk stoichiometric value [3].

The XPS data were obtained with the Tuneable High-Energy X-ray Photoelectron Spectrometer at the X-ray wiggler beam line BW2 of HASYLAB (Hamburg). The phonon flux from the Si(111) double crystal monochromator typically amounts to $5 \times 10^{12} \text{ s}^{-1}$ on the sample. The photoelectrons were measured using a hemispherical analyzer with parallel detection capability (SCIENTA SES-200). Excitation energy $h\nu = 3000$ eV was chosen, where the kinetic energy of photoelectrons from La and Ni core levels are not overlapping any of the Auger electron emission peaks. The total energy resolution at this photon energy was 0.6 eV. The binding energy (BE) scale was calibrated using the photoemission from gold reference sample. The adventitious carbon C 1s line was used for the fine correction of the charging effects, supposing that its BE should be equal to 284.6 eV.

The films were examined at different angles to distinguish between the chemical state of lanthanum and nickel at the surface and slightly deeper into the material. Angle dependent data were obtained by rotating the sample relative to the electron analyzer, which accepts electrons in the Synchrotron Radiation orbit plane at 45° relative to the incoming beam. The base pressure in the analyzer chamber was 5×10^{-10} mbar.

3. Results and discussion

X-ray photoelectron spectra from lanthanide materials exhibit the fine structure besides the main (M) spin-orbit split peaks. On the one hand, additional satellite (S) peaks complicate the elemental quantitative analysis, but, on the other hand, these fine structure parameters may be helpful in the identification of the chemical state of lanthanide ions.

As an example, the La $3d_{5/2}$ region core level spectra measured at normal ($\Theta = 0^\circ$) and grazing ($\Theta = 89.3^\circ$) take-off angles are presented in Fig. 1. The evident difference between the observed spectra obviously indicates that the

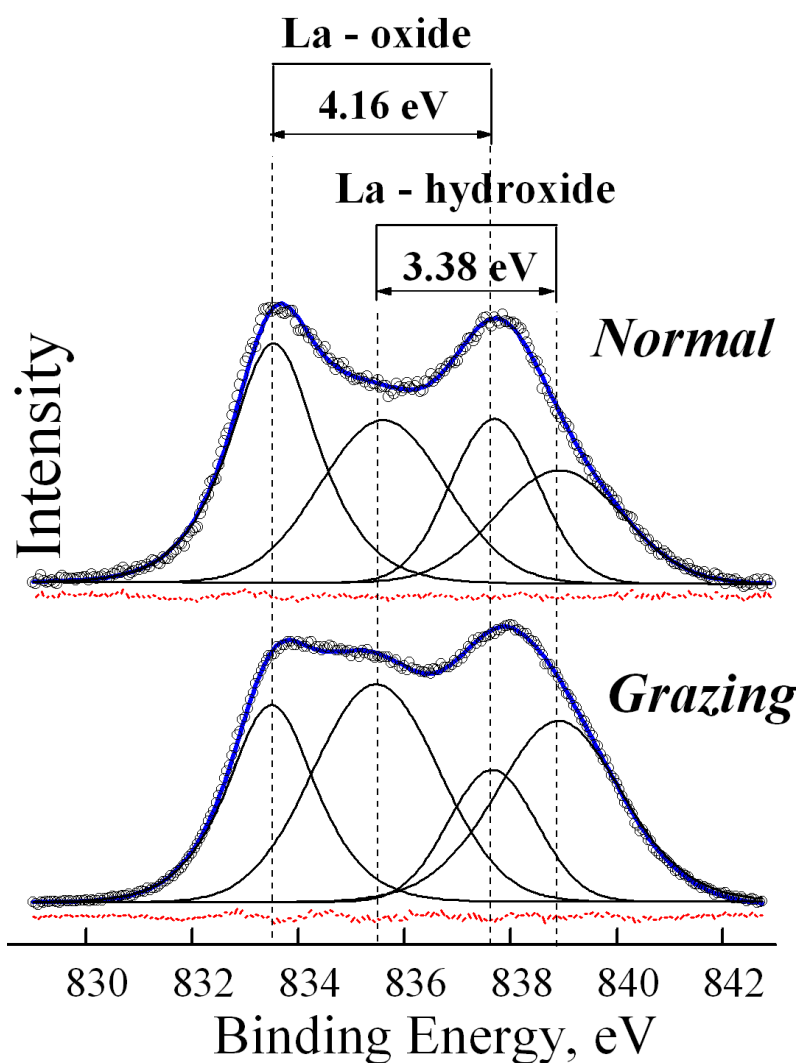


Fig. 1. XPS La $3d_{5/2}$ core-level spectra measured at normal and grazing conditions. Points refer to the raw data. Thin solid lines represent the spectral components and the thick line is the spectra envelope. Dashed lines (below) correspond to the fitting residuals.

significant alteration of the film chemical composition takes place within a thin (scanning depth ≈ 10 nm) surface layer. Both spectra may be deconvoluted into two doublets: $(M_{\text{ox}}; S_{\text{ox}})$ and $(M_{\text{hyd}}; S_{\text{hyd}})$ corresponding to the oxide and hydroxide species, respectively. Lower energy peaks M_{ox} and M_{hyd} were related with the main core-level photoelectrons, while the higher energy peaks S_{ox} and S_{hyd} — with the shake-up satellites [5, 6].

The values of the doublet splitting ($M_{\text{ox}} - S_{\text{ox}} = 4.16$ eV and ($M_{\text{hyd}} - S_{\text{hyd}} = 3.38$ eV are in agreement with those reported for La_2O_3 and $\text{La}(\text{OH})_3$, respectively [5–7]. The increase in $M_{\text{hyd}}/M_{\text{ox}}$ peaks intensities ratio in passing from normal to grazing configuration clearly indicates that the hydroxide layer is mainly located on the film surface. The hydroxide-containing phase was located near the surface, because with increasing take-off-angle an increase in the intensity ratio $R = A_{\text{hyd}}/A_{\text{ox}}$ (where A_{hyd} and A_{ox} are the areas of the M_{hyd} and M_{ox} peaks, respectively) was observed (Fig. 1).

For the LaNiO_{3-x} films, the analysis of the most intensive Ni $2p_{3/2}$ profile was complicated due to the overlapping of the Ni $2p_{3/2}$ and La $3d_{3/2}$ peaks — Fig. 2. Thus, Ni $2p_{3/2}$ core level spectra cannot be analyzed separately without La $3d_{3/2}$ spectra analysis. To overcome these difficulties the whole La $3d_{3/2}$ and Ni $2p_{3/2}$ BE region was fitted using the previously obtained results (Fig. 1) and taking into account that the contour of the envelope spectra is identical for both La $3d_{5/2}$ and La $3d_{3/2}$ components [5, 6]. Thus, only two independent parameters, i.e. spin-orbit-splitting (SOS) and La $3d_{5/2}/\text{La } 3d_{3/2}$ intensities ratio (IR), describe the resulting La $3d_{3/2}$ spectra. In spite of numerous assumptions, the procedure appears to be reasonably accurate since the estimated values of La $3d$ doublet SOS = 16.8 eV and La $3d_5/\text{La } 3d_3$ intensity ratio IR = 1.39 are in good agreement with data reported for La_2O_3 and $\text{La}(\text{OH})_3$ [6].

As in the case of La $3d_{5/2}$ line — Fig. 1 at least two kinds of nickel species with BE = 854.2 and 855.9 eV contribute to the total Ni $2p_{3/2}$ and La $3d_{3/2}$ spectrum (Fig. 2) at the film surface. These two phases may be attributed to the nickel in oxide (BE = 854.2 eV) and hydroxide (BE = 856.0 eV) state, respectively [8]. The excellent agreement between our obtained and reported in literature BE values once more corroborates the adequacy of the spectra fitting technique employed. Relative intensity of the peak corresponding to the hydroxide nickel species increases in passing from normal to grazing conditions, thus confirming that the hydroxide phase is located mainly on the film surface.

The analogous analysis of the La $4p_{3/2}$ and La $4d$ spectra also confirms the presence of both lanthanum oxide and hydroxide species on the film surface after the long time aging. For all spectral lines in question hydroxide/oxide peaks intensity ratio R strongly depends on the geometry of the experiment (Fig. 3), thus directly indicating that the thickness of the hydroxide enriched layer is of about few nanometers.

For a more quantitative analysis one requires a more or less reliable model of the hydroxide phase spatial distribution. Let us consider two specific cases:

(a) step distribution: $\rho_{\text{h}} = 1$, for $0 \leq x \leq d$, and $\rho_{\text{h}} = 0$ for $x > d$;

(b) continuous exponential distribution: $\rho_{\text{h}} = \exp(-x/d)$,

where ρ_{h} is the relative concentration of hydroxide species, and the relative concentration of oxide species $\rho_0 = 1 - \rho_{\text{h}}$.

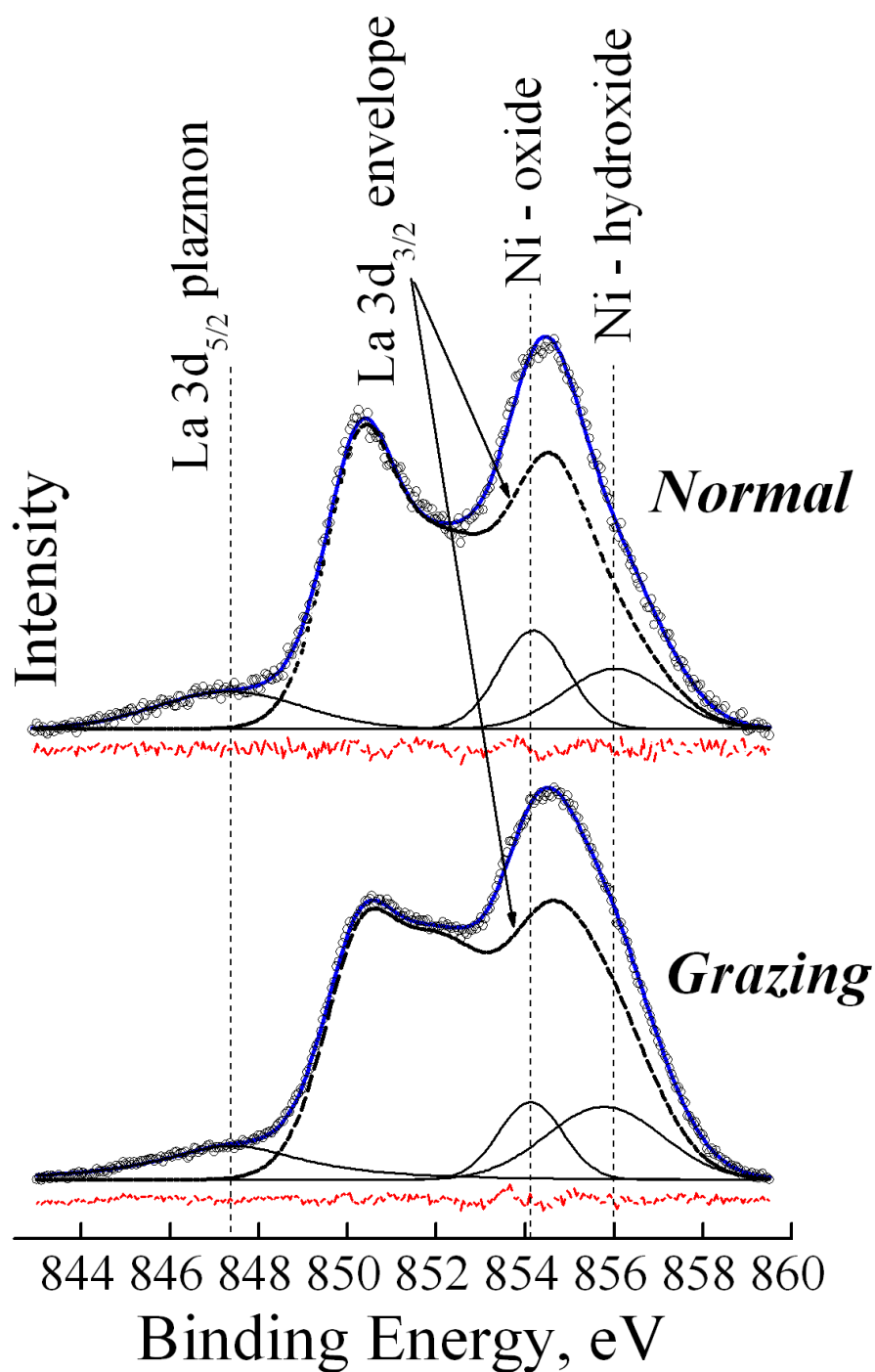


Fig. 2. XPS $\text{La } 3d_{3/2}$ and $\text{Ni } 2p_{3/2}$ core-level spectra measured at normal and grazing conditions. Points refer to the raw data. Thin solid lines represent the spectral components, the thick line is the spectra envelope and the thick dashed line (a bit lower) corresponds to the $\text{La } 3d_{3/2}$ spectra envelope. Dashed lines (below) correspond to the fitting residuals.

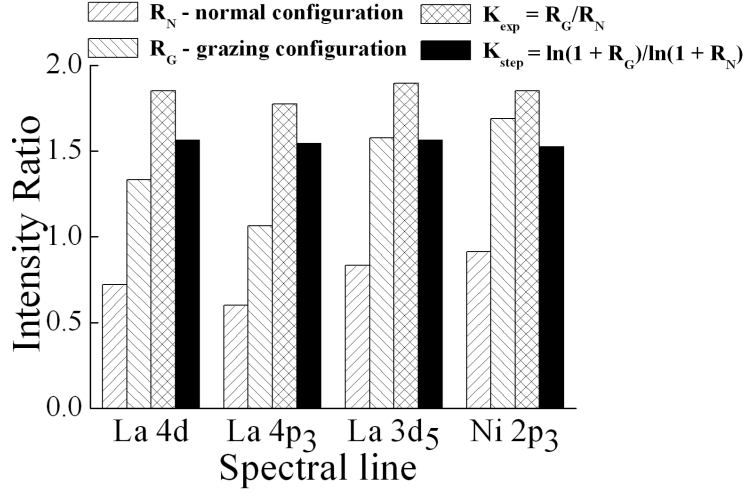


Fig. 3. Hydroxide vs. oxide peaks intensities ratio R measured at normal and grazing take-off angles and geometry factors ratio K for the “Step” and “Exponential” spatial distribution of the hydroxide species.

Then the hydroxide vs. oxide peak intensity ratio $R = I_h/I_0$, where

$$I_{h,0} = \int_0^\infty P_\theta(x) \rho_{h,0}(x) dx, \quad (1)$$

and

$$P_\theta = \frac{1}{\lambda} \exp\left(-g_\theta \frac{x}{\lambda}\right), \quad (2)$$

is the probability for a photoelectron excited at depth x to reach the surface without losing energy and be detected in θ direction, g_θ is the geometry factor depending on the experimental conditions/configuration — take-off angle, sample roughness, etc. [9], and λ is the inelastic mean free path (IMFP).

In the kinetic energy $E = (h\nu - BE)$ range $100 \text{ eV} < E < 10000 \text{ eV}$ IMFP in monolayers (MLs) may be calculated using the following semi-empirical equation [10]:

$$\lambda \approx 0.2E^{0.5}, \quad (3)$$

where λ is expressed in MLs and E in eV.

Then one obtains

$$R_\theta = \exp\left(g_\theta \frac{d}{\lambda}\right) - 1 \quad (4a)$$

and

$$R_\theta = g_\theta \frac{d}{\lambda} \quad (4b)$$

for the step and exponential distributions, respectively. Then the thickness of hydroxide layer d and geometry factors ratio $K = g_G/g_N$:

$$d = \frac{\lambda}{g_\Theta} \ln(1 + R_\Theta), \quad K = \frac{\ln(1 + R_G)}{\ln(1 + R_N)} \quad (5a)$$

and

$$d = \frac{\lambda}{g_\Theta} R_\Theta, \quad K = \frac{R_G}{R_N} \quad (5b)$$

for the step and exponential distributions, respectively.

TABLE

Core levels binding energies for oxide species at the LaNiO_{3-x} film surface and the thickness of hydroxide layer estimated for “Step” and “Exponential” distribution.

Spectral line	BE [eV]	dg_N [ML]	
		Step	Expon.
La $4d_{5/2}$	101.4	6.4	8.5
La $4p_{3/2}$	194.8	5.6	7.1
La $3d_{5/2}$	833.5	6.2	8.5
Ni $2p_{3/2}$	854.2	6.6	9.3

In the case of perfect mirror-like surface $g_\Theta = 1/\cos \Theta$, otherwise an appropriate averaging over take-off angles is required. For the normal conditions $g_N = 1$ or slightly higher. It is known that LaNiO_3 films have a smooth and crack-free surface with a surface roughness of about 2 nm [11] \approx IMFP, and the scanning depth λ/g_Θ at the grazing conditions may be estimated from the R_N/R_G ratio. It is evident from Fig. 3 and Table that in spite of great difference in BE for various spectral lines, the values of hydroxide layer thickness and geometry factors ratio estimated using Eqs. (3)–(5) are in good agreement.

4. Summary

Finally, it may be concluded that both lanthanum and nickel oxide and hydroxide species were found at the LaNiO_{3-x} film surface. The analysis of high-energy XPS spectra obtained/derived at normal and grazing conditions reveal that significant variations of oxide vs. hydroxide concentrations occur within the thin surface layer whose thickness does not exceed the XPS scanning depth even after the long time aging. The thickness of this hydroxide enriched layer was estimated from the oxide and hydroxide peak intensities ratio and taking into account that the lattice constant for $\text{LaNiO}_3 \approx 0.37$ nm [12] is of about 2 nm.

Acknowledgments

This work was done in part within the research projects 72/E-67/SPB/DESY/P-03/DWM 68/2004-20061 and EC program G1MA-CT-2002-4017 (Center of Excellence CEPHEUS) and P03B 053 26.

References

- [1] J. Choisnet, N. Abadzhieva, P. Stefanov, D. Klissurski, J.M. Bassat, V. Rives, L. Minchev, *J. Chem. Soc. Faraday Trans.* **90**, 1987 (1994).
- [2] Y. Li, N. Chen, J. Zhou, S. Song, L. Liu, Z. Yin, C. Cai, *J. Cryst. Growth* **265**, 548 (2004).
- [3] V. Bondarenka, S. Grebinskij, V. Lisauskas, S. Mickevičius, K. Šliužienė, H. Tvardauskas, B. Vengalis, *Lith. J. Phys.* **46**, 95 (2006).
- [4] V. Vengalis, A.K. Oginskas, V. Lisauskas, R. Butkutė, A. Maneikis, L. Dapkus, V. Jasutis, N. Shiktorov, in: *Thin Films Deposition of Oxide Multilayers. Industrial-Scale Processing, Proc. Int. Conf., Vilnius (Lithuania) 2000*, Eds. A. Abrutis, B. Vengalis, Vilnius University Press, Vilnius 2000, p. 45.
- [5] Y.A. Teterin, A.Y. Teterin, A.M. Lebedev, K.E. Ivanov, *J. Electron Spectrosc. Relat. Phenom.* **137-140**, 607 (2004).
- [6] D.F. Mullica, H.O. Perkins, C.K.C. Lok, V. Young, *J. Electron Spectrosc. Relat. Phenom.* **61**, 337 (1993).
- [7] H.C. Siegmann, L. Schlapbach, C.R. Brundle, *Phys. Rev. Lett.* **40**, 972 (1978).
- [8] J.C. Klein, D.M. Hercules, *J. Catal.* **82**, 424 (1983).
- [9] D. Briggs, M.P. Seach, *Practical Surface Analysis by Auger and X-ray Photoelectron Spectroscopy*, Wiley, Chichester 1983.
- [10] M.P. Seach, W.A. Dench, *Surf. Interface Anal.* **1**, 2 (1979).
- [11] F. Sánchez, C. Ferrater, X. Alcobé, J. Bassas, M.V. Carcía-Cuenca, M. Varela, *Thin Solid Films* **384**, 200 (2001).
- [12] A.Yu. Dobin, K.R. Nikolaev, I.N. Krivorotov, R.M. Wentzcovitch, E. Dan Dahlberg, A.M. Goldman, *Phys. Rev. Lett.* **63**, 113402 (2003).